Role of time-averaging of eddy covariance fluxes on water use efficiency dynamics of Maize crop

Arun Rao Karimindla, Shweta Kumari, Saipriya SR, Syam Chintala*, and BVN Phanindra Kambhammettu

Department of Civil Engineering, Indian Institute of Technology Hyderabad, Telangana, India.

*Corresponding author: E-Mail: ce22resch11012@iith.ac.in; Tel: +91 7997014429

Abstract

Direct measurement of carbon and water fluxes at high frequency makes eddy covariance (EC) as the most preferred technique to characterize water use efficiency (WUE). However, reliability of EC fluxes is largely hinged on energy balance ratio (EBR) and inclusion of low-frequency fluxes. This study is aimed at investigating the role of averaging period to represent EC fluxes and its propagation into WUE dynamics. Carbon and water fluxes were monitored in a drip-irrigated Maize field at 10 Hz frequency and are averaged over 1, 5, 10, 15, 30, 45, 60, and 120 minutes considering daytime unstable conditions. Optimal averaging period to simulate WUE fluxes for each growth stage is obtained by considering cumulative frequency (ogive) curves. A clear departure of EBR from unity was observed during dough and maturity stages of the crop due to ignorance of canopy heat storage. ~~Error~~ Deviation in representing water (carbon) fluxes relative to the conventional 30 min average is within ± 3 % (± 10 %) for 10-120 min averaging and is beyond ± 3 % (± 10 %) for other time-averages. Ogive plots conclude that optimal averaging period to represent carbon, water and WUE~~water~~ fluxes is 15-30 min for 6^{th} leaf and silking stages, and is 45-60 min for dough and maturity stages. Dynamics of WUE considering optimal averaging periods are in the range of 1.49 ± 0.95, 1.37 ± 0.74, 1.39 ± 0.79, and 3.06 ± 0.69 μmol mmol^{-1} for the 6^{th} leaf, silking, dough, and maturity stages respectively. Error in representing WUE with conventional 30 min averaging is marginal (< 1.5 %) throughout the crop period except for the dough stage (12.12 %). We conclude that the conventional 30 min averaging of EC fluxes is not appropriate for the entire growth stage. ~~Error in representing WUE with conventional 30 min averaging is marginal (< 1.5 %) except during the dough stage (12.12 %).~~ Our findings can help in developing efficient water management strategies by accurately characterizing WUE fluxes from the EC measurements.

Keywords: Eddy covariance, Maize crop, Time-average, Energy balance ratio, Ogive function, Water use efficiency.

Research Highlights:

1. The time-averages that yield the most effective energy balance closure are identified as 45 and 60 minutes.
2. Insufficiently short time-averages such as 1 and 5 minutes, as well as excessively long-time-averages such as 120 minutes, resulted in a high relative error in representing carbon and water fluxes.
3. The conventional 30-minute averaging period proved to be insufficient in capturing low-frequency fluxes, necessitating the use of longer averaging periods.
4. ~~4.~~ 4. Different time averaging periods are to be considered to compute the EC fluxes considering the crop growth stage. ~~Time-averaging of Eddy Covariance fluxes needs to be performed in accordance with crop growth stage.~~

1.0 INTRODUCTION

Water use efficiency (WUE) is an important eco-hydrologic trait relating two important processes of plant metabolism namely carbon fixation (via photosynthesis) and water consumption (via transpiration) (Bramley, 2013). The need for achieving food security with diminishing water resources under changing climate has made WUE as the controlling parameter in planning and design of irrigation strategies (Tang, 2015). Depending on the scale of investigation, WUE can be quantified at: i) leaf, ii) plant, iii) ecosystem, or iv) regional scales (Medrano, 2015). Of these, ecosystem WUE has taken precedence in irrigation and agronomy due to: i) accurate and reliable measurement using micrometeorological techniques, ii) ability to evaluate the role of various water conservation techniques on ecosystem productivity, and iii) understand the relation between carbon and water cycles in response to changes in climate (Tang, 2015; Tong, 2014).

Eddy covariance (EC) is a non-destructive, micrometeorological technique for direct measurement of water vapour (H_2O) and carbon (CO_2) fluxes between vegetation and atmosphere at high temporal frequency (Aubinet, 1999; Leclerc and Foken, 2014). EC method precisely measures the overall transfer of heat, mass, and momentum between the earth's surface (such as vegetation) and the atmosphere. This is achieved by estimating the covariance of turbulent fluctuations in vertical wind (referred to as eddies) with respect to the specific flux under consideration such as H_2O, CO_2, temperature. EC represents the scalar fluxes of interest (representative of eco-hydrological processes) from a region upwind of the measurement known as the footprint. At ecosystem scale, WUE is estimated as the ratio of net primary product (NPP: proxy for photosynthesis) to evapotranspiration (ET: proxy for water consumption) ~~WUE is estimated as the ratio of net primary product (NPP): proxy for photosynthesis to evapotranspiration (ET): proxy for water consumption~~ (Peddinti, 2020). WUE is a key eco-hydrologic trait that is used to analyse the role of climate change, drought, deficit irrigation, and management strategies on ecosystem productivity. Currently, EC is the most accurate and reliable method for estimating carbon and water ~~fluxes~~exchnages, hence WUE at ecosystem scale (Tong, 2009). A number of studies have demonstrated the efficacy of EC in estimating WUE across a wide range of ecosystems (Tang, 2015; Tong, 2014; Wang, 2017). Error sources that affect the accuracy of EC fluxes are grouped into: i) Unrepresentative (due to footprint heterogeneity, unsatisfied underlying theory), ii) Measurement uncertainties (due to random errors, interference and contamination, sensor drifts) and iii) Measurement biases in fluxes (tilt, frequency losses, air density fluctuations etc.). Despite improvements in measurement accuracy, data sampling, and processing techniques, EC method still suffers from the drawback of lack of conservation among the energy terms, resulting in energy balance closure (EBC) problem (Charuchittipan, 2014; Foken, 2011; Reed, 2018). Lack of EBC as observed in EC system is reported across diverse ecosystems ranging from simple bare soils (Oncley, 2007), to homogeneous grasslands (Twine, 2000), to heterogeneous croplands (Peddinti and Kambhammettu 2019), to complex forest ecosystem (Charuchittipan, 2014; Wilson, 2002). Apart from the errors associated with instrumentation, measurement, and neglected energy sinks, lack of EBC at the EC sites is also attributed to the omission of low frequency secondary circulations in the turbulent flux estimation (Wilson, 2002). This problem can be circumvented by choosing appropriate averaging period during flux estimation, the selection of which is based on: i) 'ensemble block time-averaging method' (Finnigan, 2003; Malhi, 2004; Sakai, 2001), and ii) 'ogive method' (Berger, 2001).

A number of studies have highlighted the importance of averaging period in quantifying the EC fluxes, with an objective to obtain optimal time-averaging period under various canopy and surface roughness conditions. While smaller averaging periods (15-30 min) are suitable for managed croplands, flux estimation from forest and tall canopies demand longer averaging periods (60-120 min) due to the presence of large-sized, slow moving eddies (Finnigan, 2003;

Sakai, 2001; Sun, 2006). Zhang (2013) concluded that time-averaging of EC fluxes has to be done in accordance with the observation scale. In an analysis of Chengliu riparian forest in China, they found that lower time-averaging periods (15 min) are suitable for daily variation of EC fluxes, whereas higher time-averaging periods (60 min) are suitable for long-term flux computations. A similar observation was made by Lee (2004) over farmlands. In a wheat field in Yucheng, China, 10 min and 30 min averaging periods were found suitable for diurnal and long-term flux observations respectively. Flux observations over a Maize crop at Daxing experimental station in China conclude that optimal time-averaging period has to be considered in accordance with crop growth stage (Feng, 2017). However, they observed a marginal (< 3 %) error in representing the fluxes at conventional 30 min averaging relative to the optimal averaging obtained for each growth stage.

Maize is the third most important cereal crop in India after rice and wheat, and accounts for about 10 % of total food production in the country (Sharma, 2018; Ficci 2014). Inspite of a huge area under cultivation (9.4 MHa), high production (23 million tons), and enormous water consumption (18 BCM), both crop productivity (2.5 t ha^{-1}) and crop water productivity~~:~~ (CWP) (1.83 kg m^{-3}) of Indian Maize are far lower than corresponding world averages (Sharma, 2018). Low CWP (hence, WUE) of Indian Maize can be attributed to: i) a high dependence (85 %) on erratic, uncertain rainfall, ii) low adoption of hybrid varieties, iii) improper drainage facilities leading to water logging, and iv) unscientific application of irrigation water without analysing soil-water-crop interactions (Shankar, 2012). Thus, an accurate quantification of WUE and its temporal variation during the crop cycle is essential for effective irrigation water management of Maize crop (Medrano, 2015).

While the effect of time-averaging on carbon and water fluxes measured at EC sites is reported, the effect on their interaction term, i.e. WUE, which is crucial in irrigation water management is unexplored. Evaluation of time-averaging period on WUE dynamics is necessary to understand the contribution of low and high frequency photosynthetic carbon and evaporative water fluxes generated from various field management strategies. Also, most of the EC flux studies are confined to data rich AmeriFLUX, EuroFLUX, and ChinaFLUX sites, with limited focus to Indian fragmented croplands. This motivates the present study, and the objectives of this study are as follows: i) investigate the role of time-averaging of EC fluxes on EBR and WUE dynamics, ii) compute optimal averaging period to simulate carbon and water (hence, WUE) fluxes of Maize crop, and iii) investigate the association of carbon, water, and WUE fluxes between multiple averaging periods. Results of this study can help in designing efficient management strategies using EC datasets in response to changes in WUE during the crop cycle.

2.0 MATERIALS AND METHODOLOGY

2.1 Site Description and Instrumentation

Controlled Maize plots situated at Professor Jaya Shankar Telangana State Agricultural University (PJTSAU), Hyderabad, Telangana, India (17°19′17″ N, 78°24′35″ E, 559 m above sea level) forms the study area. The region is composed of red gravel to sandy loam soils with field capacity and wilting point in the ranges of 17.92 - 19.56 % and 8.2 – 9.87% respectively. As per Koppen-Geiger's classification, the region falls under tropical savanna climate zone (Aw) characterized by long dry and short wet seasons (Kottek, 2006). Mean annual precipitation of the region is 900 mm (IMD, 2019) with more than 80% occurring during the monsoon months (Jun-Sep). Temperatures are high during summer (38.33 ± 2.12 ~~^{0}C~~°C) and low during winter (30 ± 2.20 ~~^{0}C~~°C) months. Humidity of the region varies from 35% in summer to 73% in monsoon (CGWB, 2013). Mean seasonal wind speed is in the range of 1.5 to 2.7 m/s (Peddinti and Kambhammettu 2019). Hydro-geologically, the study area forms part of the Deccan plateau characterized by multiple layers of solidified flood basalt resulting from volcanic eruptions. Depth to groundwater ranges from 12 m (pre-monsoon) to 6 m (post-monsoon) (CGWB, 2013).

Meteorological parameters and turbulent fluxes were obtained for one crop season, i.e. 26 May to 06 Sep, 2019 using an open path eddy covariance (EC) flux tower. The flux system is composed of integrated CO_2/H_2O open-path gas analyzer and 3D sonic anemometer (IRGASON-EB-NC, Campbell Sci. Inc., USA) to measure CO_2 and H_2O concentrations at 3 m above the canopy. ~~The flux system is composed of a 3D sonic anemometer (CSAT3, Campbell Sci. Inc., USA), and an open-path fast response infrared gas analyzer (IRGASON-EB-IC, Campbell Sci. Inc., USA) to measure~~ ~~CO_2~~ ~~and~~ ~~H_2O~~ ~~fluxes at 3 m above the canopy.~~ Raw data was collected with a logger (CR1000, Campbell Sci. Inc., USA) at 10 Hz frequency. Additionally, slow response meteorological variables including precipitation (TE525-L-PTL, Tipping Bucket, Campbell Sci. Inc., USA), soil heat flux (HFP01SC-L-PTL, Campbell Sci. Inc., USA), solar radiation (CNR 4, Campbell Sci. Inc., USA), and soil moisture (CS616-L-PT-L, Campbell Sci. Inc., USA) were obtained at 10 min intervals.

Formatted: Not Highlight

2.2 Data Collection and Processing

Table 1 shows the phenological stages of the Maize crop in the study area (Soujanya, 2021). Additionally, leaf-area index (LAI) and mean plant height were ~~measured~~ monitored during the crop cycle (Table 1). The LAI was measured using the plant canopy analyser, whereas the plant height was measured using a ruler from the base of the plant to its crown. Maize crops of the experimental fields are sown on 25th May 2019 and harvested on 6th September 2019 with a base period of 104 days.

Table 1: Phenological growth stages and physical properties of the Maize crop

S. No.	Growth stage	Start date	End date	Period Length (days)	Leaf Area Index (m^2m^{-2})	Plant height (cm)
1	6th leaf	26/05/2019	12/06/2019	18	0.61	46.8
2	Silking	13/06/2019	19/07/2019	37	1.56	75.2
3	Dough	20/07/2019	12/08/2019	24	3.46	133
4	Maturity	13/08/2019	06/09/2019	25	3.03	134

Data from the EC system at 10 Hz frequency was converted to ASCII format using LoggerNet (4.3) software (Campbell Scientific Inc., Logan, Utah, USA), and further aggregated to various averaging periods (1, 5, 10, 15, 30, 45, 60, and 120 minutes). Post data processing was done using EddyPro post-processing software (version 7.0.8, LI-COR, USA). Primary corrections performed on the raw dataset include tilt corrections, turbulent fluctuations, density fluctuations, frequency corrections and quality checks. Tilt corrections were made by the double axis rotation method for each averaging period. Either~~The~~ block average method or ~~an~~d linear ~~de~~trending method were ~~used~~ considered to ~~correct~~ compute the turbulent fluctuations. Block averaging method was used for detrending the fluxes at 1, 5, 10, 30, 45, and 60 min averaging periods. Longer averaging periods (e.g. 120 min) has resulted in inconsistency in the obtained fluxes, which is a weakness of the block averaging (Renhua,

Formatted: Not Highlight

Formatted: Not Highlight

2005; Sun et al., 2006). Hence, linear trend removal method was used to compute the fluxes for 120 min averaging period. Density fluctuation corrections were done using Webb–Pearman–Leuning (WPL) method. Quality checks were performed following a flagging policy proposed by Mauder and Foken (2006) (0-1-2 system). Flag set to "0" corresponds to the best quality fluxes, "1" corresponds to fluxes acceptable for general analysis, and "2" corresponds to poor quality fluxes that should be removed from the dataset. The resulting fluxes may exhibit spikes, discontinuity, randomness etc. There is a need to perform secondary corrections on the data that include flux spike removal (Vickers and Mahrt 1997), friction velocity corrections (to filter night time observations), gap filling and uncertainty analysis (Finkelstein, 2001), skewness & kurtosis removal, spectral corrections, and frequency corrections. To correct flux estimates for low and high frequency losses due to instrument setup, intrinsic sampling limits of the devices, and various data processing decisions, spectral corrections are performed. Additionally, slow sensor meteorological data obtained at 1 min interval were processed for different time-averaging periods using the EddyPro post-processing software (version 7.0.8, LI-COR, USA).

Formatted: Not Highlight

2.3 Effect of time-averaging on EBR and EC fluxes

Violation of law of conservation of energy resulting from the EC observed energy terms is referred as energy balance closure (EBC). ~~Lack of conservation among the measured energy terms of the EC tower is referred as energy balance closure (EBC).~~ The available energy (R_n-G) is generally higher than the turbulent fluxes (H+LE), resulting in a positive balance (Eshonkulov, 2019) where R_n, G, H and LE correspond to net radiation, soil heat flux, sensible heat and latent heat respectively. Apart from instrument and measurement issues, this lack of energy closure is thought to be partly from averaging periods and coordinate systems (Finnigan, 2003; Finnigan, 2004; Gerken, 2018). The energy closure fraction, commonly termed as energy balance ratio (EBR) is used to evaluate the quality of EC data by examining energy fluxes at the surface (Chen and Li 2012), given by:

Formatted: Not Highlight

$$EBR = \frac{H+LE}{R_n - G} \quad (1)$$

$$H = \rho_a C_p \overline{w'T'} \quad (2)$$

$$LE = L_v \overline{w'\rho_v'} \quad (3)$$

Formatted: Font: 12 pt, Italic

Formatted: Font: 12 pt, Italic, Font color: Dark Blue

Formatted: Font: 12 pt, Font color: Dark Blue

Formatted: Normal, Indent: Left: 0 cm

where ρ_a is the air density; C_p is the specific heat of air, w' is the wind velocity fluctuation, T' is the temperature fluctuation, L_v is the latent heat of vaporization and ρ_v' is the H_2O gas concentration fluctuation.

EBR helps to determine the averaging period required to calculate H and LE fluxes over a range of landscapes (Chen and Li 2012). A high EBR (EBR ≥ 0.7) ensures reliability of EC observations for use with flux estimation (Barr et al., 2006; Kidston et al., 2010).

Eddy fluxes are computed as the covariance between instantaneous deviation in vertical wind speed (w') and scalar component of interest (s') from their respective means, given by

$$\mathrm{F} \approx \overline{\rho_a w' s'}$$

(~~2~~4)

where $\overline{\rho_a}$ is the mean air density, and the overbar represents the time-average of eddy fluxes, which is of interest in the present study. Depending on the scalar component considered (ex: temperature, water vapour (H_2O), carbon dioxide (CO_2) concentration), corresponding eddy fluxes (ex: sensible heat, latent heat, carbon flux) are computed as below.

$$F_{CO_2} \approx \overline{\rho_a w' CO_2{}'} \qquad (\cancel{3}5)$$

$$F_{H_2O} \approx \overline{\rho_a w' H_2O'} \qquad (\cancel{4}6)$$

Ecosystem WUE is then estimated as the ratio of daytime carbon (net primary product) to water fluxes (evapotranspiration), observed ~~during~~ considering daytime unstable atmospheric conditions (08:00 am to 04:00 pm) given by:

$$WUE = \frac{NPP}{ET} = \frac{F_{CO_2}}{F_{H_2O}} \qquad (5)$$

Fluxes originating from real-world sites are composed of both high frequency (turbulence) and low frequency (advection) fluctuations, with a spectral gap in between. Isolating local turbulence component for use with flux studies is achieved by choosing an appropriate averaging period, T_1 (typically 30 minutes) on fast response measurements operating at high frequency T_2 (Manon and Kristian 2020). Optimal averaging period (T_1) should be long enough to reduce random error (Berger, 2001) and short enough to avoid non-stationarity associated with advection (Foken & Wichura, 1996). The flux estimates (eq. 2) are further decomposed

Formatted: Font: (Default) Times New Roman, 12 pt

Formatted: Font: (Default) Times New Roman, 12 pt, Font color: Dark Blue

Formatted: Font: (Default) Times New Roman, 12 pt, Font color: Dark Blue

Formatted: Font: 12 pt, Font color: Dark Blue

Formatted: Font: (Default) Times New Roman, 12 pt, Font color: Dark Blue

Formatted: Font: (Default) Times New Roman, 12 pt, Font color: Dark Blue

Formatted: Font: 12 pt, Font color: Dark Blue

Formatted: Font: 12 pt, Font color: Dark Blue

Formatted: Font: (Default) Times New Roman, 12 pt, Font color: Dark Blue

Formatted: Font: (Default) Times New Roman, 12 pt, Font color: Dark Blue

Formatted: Font: (Default) Times New Roman, 12 pt, Font color: Dark Blue

Formatted: Font: (Default) Times New Roman, 12 pt, Font color: Dark Blue

Formatted: Font: 12 pt, Font color: Dark Blue

Formatted: Font: (Default) Times New Roman, 12 pt, Font color: Dark Blue

Formatted: Space Before: 0 pt, After: 8 pt

Formatted: Font: (Default) Times New Roman, 12 pt, Font color: Dark Blue

Formatted: Font: (Default) Times New Roman, 12 pt, Font color: Dark Blue

Formatted: Font: (Default) Times New Roman, 12 pt, Font color: Dark Blue

Formatted: Font: 12 pt, Font color: Dark Blue

Formatted: Font: 12 pt, Font color: Dark Blue

Formatted: Font: (Default) Times New Roman, 12 pt, Font color: Dark Blue

Formatted: Subscript

Formatted: Font: (Default) Times New Roman, 12 pt, Font color: Dark Blue

Formatted: Font: (Default) Times New Roman, 12 pt, Font color: Black into frequency dependent contributions, known as co-spectra Co_{ws} (f) between vertical wind velocity (w) and scalar of interest (s) for frequencies 'f' (Manon and Kristian 2020). For an accurate estimation of the flux, it is essential that the EC method is applied under conditions where the flow is stationary, and all eddies carrying flux are sampled. Given that the flow remains stationary, an 'ogive' serves as a check for the essential requirement to sample all scales carrying the flux. Ogive function is well proposed to check if all low frequency fluxes are included in the turbulent flux measured with the EC method (Foken & Wichura, 1996; Foken et al., 2005). It is used to investigate the energy balance losses caused by low frequency fluxes. Ogive analysis is performed to investigate the flux contribution from each frequency range and to arrive at most suitable averaging period to capture most of the turbulent fluxes (Desjardans, 1989; Charuchittipan, 2014). Ogive function thus provides the cumulative sum of co-spectral energy starting from the highest frequency, given by:

$$Og_{ws}(f_0) = \int_{f_0}^{\infty} \mathrm{Co}_{ws}(f)\,\mathrm{d}f \qquad (\cancel{6}7)$$

The point of convergence on the Ogive plot to an asymptote corresponds to optimal averaging period (T_1) for use with averaging of high frequency turbulence fluxes. In other words, the point at which the ogive plot flattens out represents the optimal averaging period. A total of eight averaging periods, i.e., 1, 5, 10, 15, 30, 45, 60, and 120 minutes were considered to investigate the role of time-averaging on EBR, EC and WUE~~ and EC~~ fluxes, and further to arrive at the optimum averaging period for use with WUE estimation. The biophysical and physiological characteristics such as plant height, crop water requirement, LAI, etc. changes with respect to the crop growth stage (Chintala et al., 2024) and have a significant effect on the EC fluxes. Since these factors vary over growth stages, ~~For this reason,~~ time-averaging of EC fluxes is separated based on crop growth stage.

2.4 Performance Evaluation

The ability of various averaging periods to close the energy balance and compute the EC fluxes is evaluated using three goodness of fit indicators, namely: a) coefficient of determination (R^2), b) root mean squared error (RMSE), and c) relative error (RE). While R^2 and RMSE aim to quantify the error in closing the energy balance, RE is aimed to compute the error in estimating EC fluxes with conventional 30 min averaging period relative to optimal averaging period.

Root mean square error (RMSE) measures overall accuracy in closing the energy balance for a given averaging period by penalizing large errors heavily, given by:

$$\cancel{RMSE = \left[\frac{\sum_{i=1}^{n}(R_n-G)_i-(H+LE)_i}{n}\right]^{0.5}}$$

$$RMSE = \left[\frac{\sum_{i=1}^{n}\left((R_n-G)_i-(H+LE)_i\right)^2}{n}\right]^{0.5} \qquad (\cancel{7}8)$$

~~Where~~ where n is the number of observations.

Coefficient of determination (R^2) and Pearson correlation coefficient (r) ~~is~~ are the~~a~~ measures of the strength of linear association between turbulent fluxes and available energy, given by:

$$R^2 = \left\{\frac{\sum_{i=1}^{n}\left[(R_n-G)_i-\overline{(R_n-G)}\right]^2\left[(H+LE)_i-\overline{(H+LE)}\right]^2}{\sqrt{\sum\left[(R_n-G)_i-\overline{(R_n-G)}\right]^2\left[(H+LE)_i-\overline{(H+LE)}\right]^2}}\right\}^2 \qquad (\cancel{8}9)$$

$$r = \left\{\frac{\sum_{i=1}^{n}\left[(R_n-G)_i-\overline{(R_n-G)}\right]\left[(H+LE)_i-\overline{(H+LE)}\right]}{\sqrt{\sum\left[(R_n-G)_i-\overline{(R_n-G)}\right]^2\left[(H+LE)_i-\overline{(H+LE)}\right]^2}}\right\}$$

Relative error (RE) provides the disparity in the fluxes estimated with conventional (30 min) relative to the fluxes estimated with optimal averaging period, given by:

$$RE = \left[\frac{\{F_{opt}-F_{30min}\}}{F_{opt}}\right] \times 100 \qquad (\cancel{9}10)$$

where F_{opt} and F_{30} are the flux of interest considering optimal and conventional (30 min) averaging periods.

Averaging period corresponding to ~~A~~ high R^2 (close to 1), low RMSE (close to zero)~~, and low RE (close to zero)~~ is considered to be the optimal choice in representing the EC fluxes.

3.0 RESULTS AND DISCUSSION

3.1 Diurnal variations in energy balance components

To understand the energy variation in response to rapid changes in meteorological conditions, we analysed the diurnal variations in energy balance components. Figure 1 shows

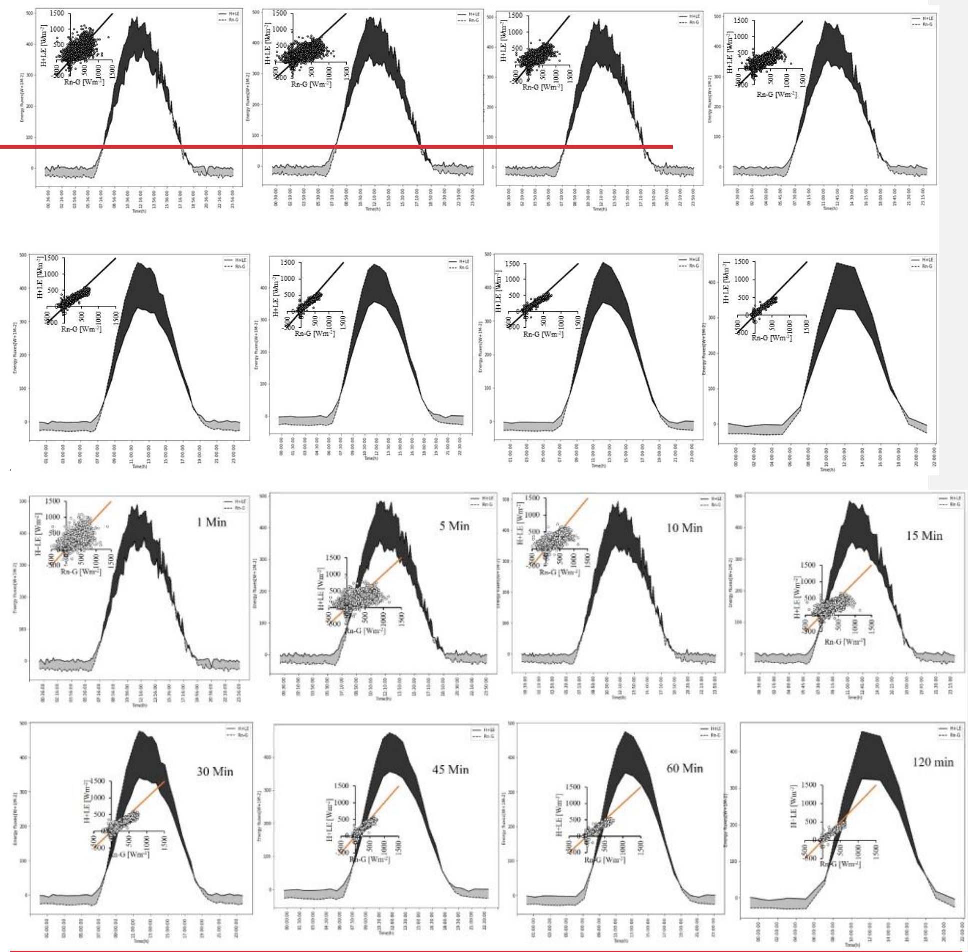

Figure 1: Diurnal variations in energy balance components (available energy: R_n-G and turbulent fluxes: H+LE) during the crop cycle with different averaging periods. Inset: Scatter-plots between the two datasets.

the diurnal variations in available energy (R_n-G) and turbulent fluxes (H+LE) averaged over the crop cycle for various time-averages. The diurnal variations of (R_n-G) and (H+LE) are bell-shaped, with peak occurring at around noon (480.16 ± 14.15 Wm^{-2}, 356.23 ± 18.51 Wm^{-2}) (Figure 1). The energy balance difference (shaded areas of the figure) is found to be positive (76.88 ± 43.14 Wm^{-2}) during daylight hours (08:00 am to 06:00 pm) and is negative (-24 ± 11.65 Wm^{-2}) for the remaining time. The vertical offset between the two curves, representing the residual of energy balance is highest around the noon (142.39 ± 19.42 Wm^{-2}), and is consistent between the averaging periods. For an average site-day, the cumulative energy balance difference was found to be constant with a mean of 1811 ± 91.56 Wm^{-2} at all averaging periods. The cumulative energy balance difference is crossing the 'zero' line at around 11:30 am. The variation is rough at lower averaging periods due to a high sample size (n= 10859 at T = 1 min) and is gradually smoothened towards higher averaging periods (n= 811 at T = 120 min). The slope of regression lines between (H+LE) and (R_n-G) considering all averaging periods are in the range of 0.59 to 0.71 with a mean of 0.65 ± 0.041. The intercept is ranged from 19.01 to 31.56 Wm^{-2}. The best slope (≥ 0.70) and intercept (≤ 20 Wm^{-2}) were achieved with 45 and 60 minutes averaging periods, which is consistent with literature (Gao, 2017; Leuning, 2012). This conclude that, longer averaging periods have a good closure over shorter averaging periods. The strength of linear association between (R_n-G) and (H+LE) around the best fit line, explained by *r* is high ($0.80 < r \leq 0.9$) at low averaging periods, i.e., 1, 5, 10 minutes, and is very high ($r > 0.9$) for other averaging periods (Table 2). However, the departure of the data from 1:1 line is relatively low both at ~~low~~ short and ~~high~~ long averaging periods. Our findings show that averaging period has minimal influence in representing the energy balance terms. However, data scatter around 1:1 line is high for shorter time-averages due to large sample size and data randomness. ~~Our findings show that averaging period has minimal influence in representing the energy balance terms.~~

Formatted: Not Highlight

Table 2: Summary of linear regression parameters in closing the energy balance with different averaging periods.

Averaging Period	Slope	R^2	Intercept (Wm^{-2})	r	N	RMSE (Wm^{-2})
1min	0.63	0.66	30.31	0.81	10859	98.38
5min	0.59	0.74	31.56	0.86	10785	76.47
10min	0.60	0.80	28.94	0.90	10753	64.41
15min	0.63	0.84	26.56	0.92	7150	58.18
30min	0.66	0.93	20.49	0.96	3554	38.33
45min	0.70	0.94	19.99	0.97	2355	36.30

60min	0.71	0.94	19.01	0.97	1765	35.07
120min	0.67	0.93	20.77	0.96	811	39.95

3.2 Effect of averaging period on EBR and EC fluxes

The variation in energy balance ratio (EBR) with averaging period for individual growth stages of the crop is presented in Figure 2. We observed a clear departure of EBR from

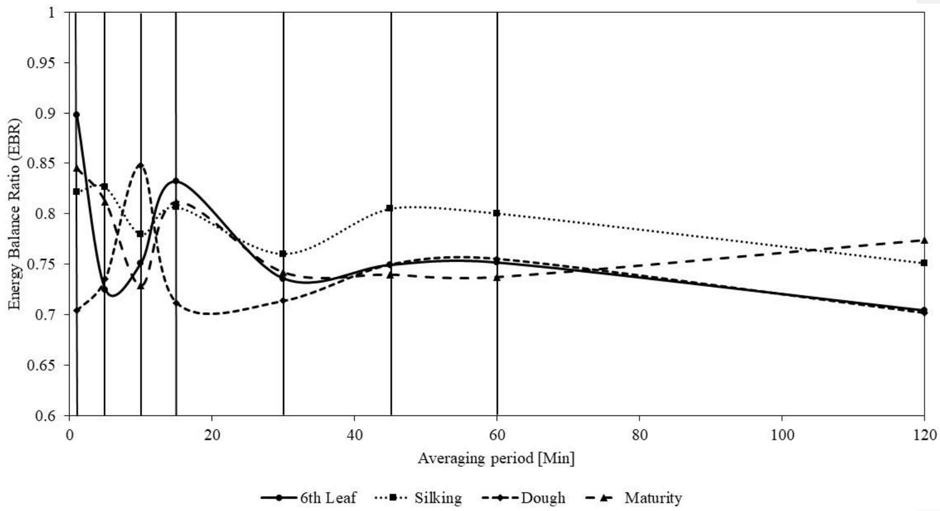

Figure 2: Variation in energy balance ratio (EBR) with averaging period for different growth stages. (Solid verticals from left to right correspond to the averaging periods of 1 min, 5 min, 10 min, 15 min, 30 min, 45 min, 60 min, and 120 min respectively).

unity for all growth stages, particularly with dough and maturity stages due to ignorance of canopy heat storage. EBR is fluctuating between 0.70 and 0.90 at low (1 – 30 min) averaging periods and is fairly constant (0.75 ± 0.03) at high (≥ 30 min) averaging periods. Our reported values of EBR during the crop growth are within the typically found range of 0.65 to 1.2 for most of the crops (Feng, 2017; Finnigan, 2003; Wilson, 2002). The mean EBR with conventional 30 min averaging period is found to be 0.74, 0.76, 0.71, and 0.74 during 6th leaf, silking, dough, and maturity stages respectively. Low EBR during the crop cycle can also be attributed to the ignorance of energy transport associated with large eddies from landscape heterogeneity. However, EC method assumes the landscape within the footprint of measurement to be flat and homogenous. This violation might have lowered the EBR.~~Low~~

Formatted: Not Highlight

~~EBR during the crop cycle can also be attributed to the ignorance of energy transport associated with large eddies from landscape heterogeneity, which is not captured by the EC system~~. We could not observe any significant differences in temporal trends of 'wind speed' and 'wind direction' between the averaging periods, hence meteorological conditions were not analysed by varying time-average. Changes in daytime mean carbon and water fluxes with averaging period for different growth stages of the crop is shown in Figure 3. Carbon fluxes (sink) have a very low mean (1.81 ± 0.06 µmol $m^{-2}s^{-1}$) during 6^{th} leaf stage, low mean during silking (3.48 ± 0.07 µmol $m^{-2}s^{-1}$) and dough (3.03 ± 0.87 µmol $m^{-2}s^{-1}$) stages, and a high mean (15.44 ± 0.75 µmol $m^{-2}s^{-1}$) during maturity stage.

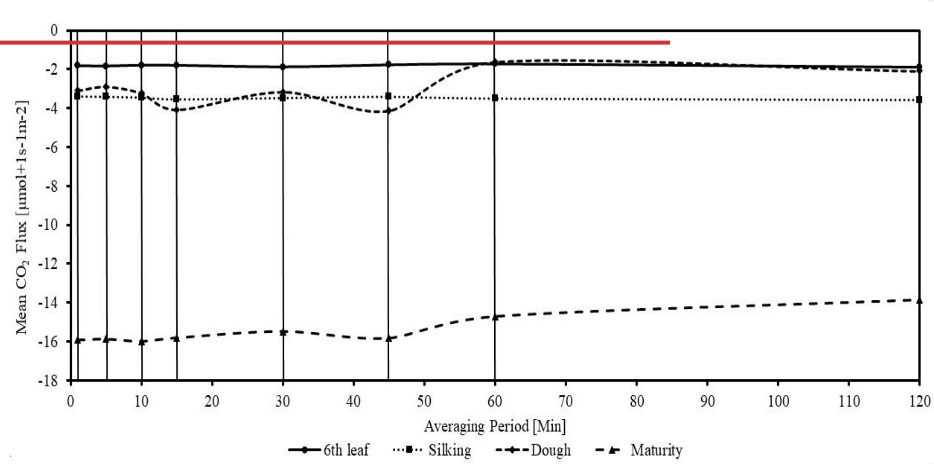

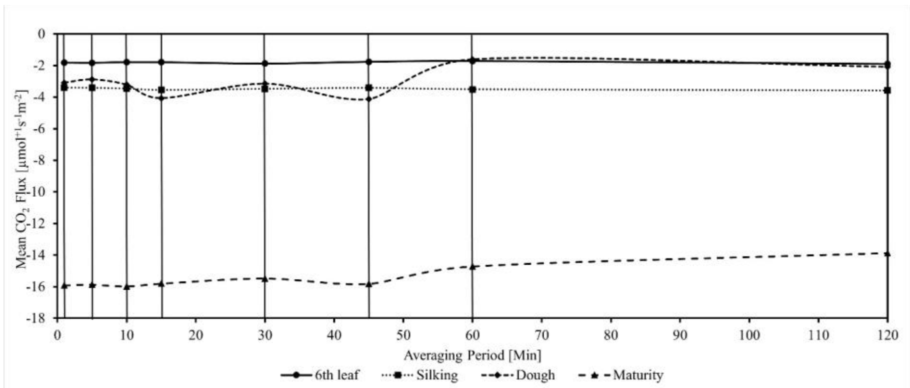

Figure 3a: Variation in mean carbon fluxes with averaging period for different growth stages (Solid verticals from left to right correspond to the averaging periods of 1 min, 5 min, 10 min, 15 min, 30 min, 45 min, 60 min, and 120 min respectively).

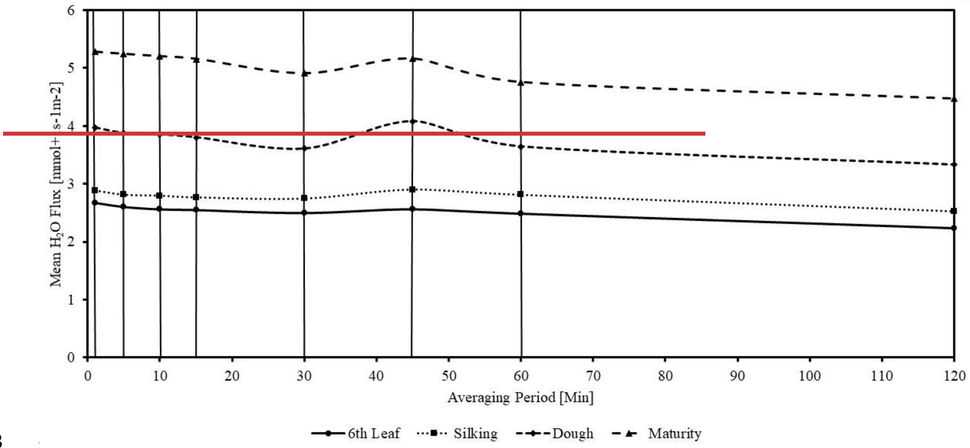

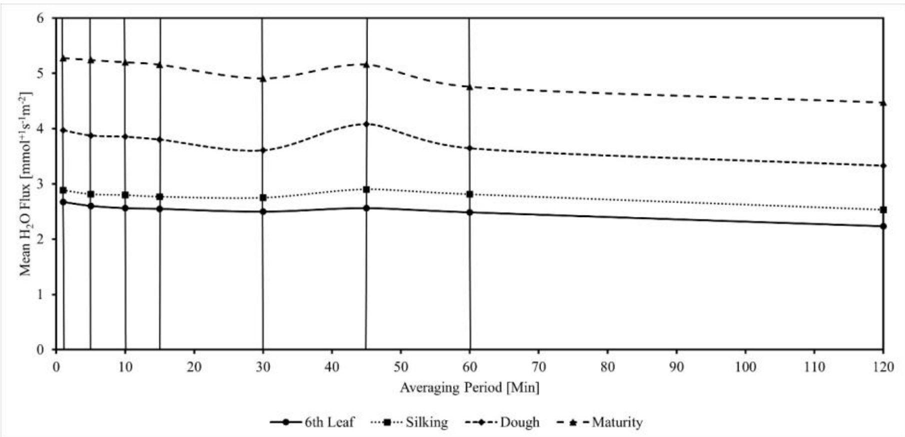

Figure 3b: Variation in mean water fluxes with averaging period for different growth stages (Solid verticals from left to right correspond to the averaging periods of 1 min, 5 min, 10 min, 15 min, 30 min, 45 min, 60 min, and 120 min respectively).

~~low mean during silking (3.48 ± 0.07 µmol·m^{-2}s^{-1}) and dough (3.03 ± 0.87 µmol·m^{-2}s^{-1}) stages, and a high mean (15.44 ± 0.75 µmol·m^{-2}s^{-1}) during maturity stage~~. Mean carbon fluxes during 6th leaf and silking stage are mostly unaffected by averaging period. We observed a gradual increase in water vapour fluxes during the crop cycle~~,~~ from 6th leaf (2.52 ± 0.13 mmol s^{-1}m^{-2}) to maturity (5.02 ± 0.29 mmol s^{-1}m^{-2}). As the averaging period is increased, the mean water vapour flux is decreased, with an exception at 45 min averaging period. ~~Distribution of error~~Deviation in in representing carbon and water fluxes at different averaging periods, relative to the conventional 30 min averaging period i.e. relative error (RE) is presented in Figure 4. The RE is obtained by considering daily averages in the deviations for each growth

Formatted: Not Highlight

Formatted: Not Highlight

stage. During 6th leaf and silking stages, RE in estimating carbon fluxes is high (~ -15 %) with low averaging periods, and is gradually diminishing towards higher averaging periods, with an exception at very high (120 min) average period. For dough and maturity stages, RE is found to be significant with higher averaging periods (60-120 min). RE in estimating water vapour fluxes is found to be insignificant at all averaging periods for the 6th leaf and silking stages. However, dough and maturity stages have shown a large variation in RE considering either too-short (1, 5 min) or too-long (60, 120 min) time averages. A high variability in RE for time scales larger than 45 min indicate the effects of sub mesoscale (non-turbulent) motions. Hence, 45 min average period can be considered as optimal in isolating the turbulence components for use with flux representation. ~~RE in estimating water vapour fluxes is found to be insignificant at all averaging periods, irrespective of growth stage~~.

Formatted: Not Highlight

Formatted: Not Highlight

Formatted: Not Highlight

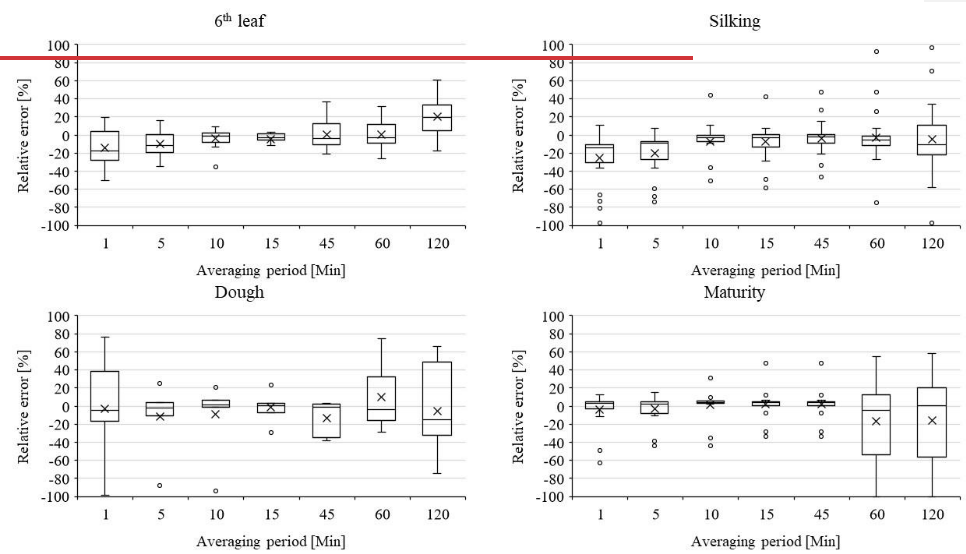

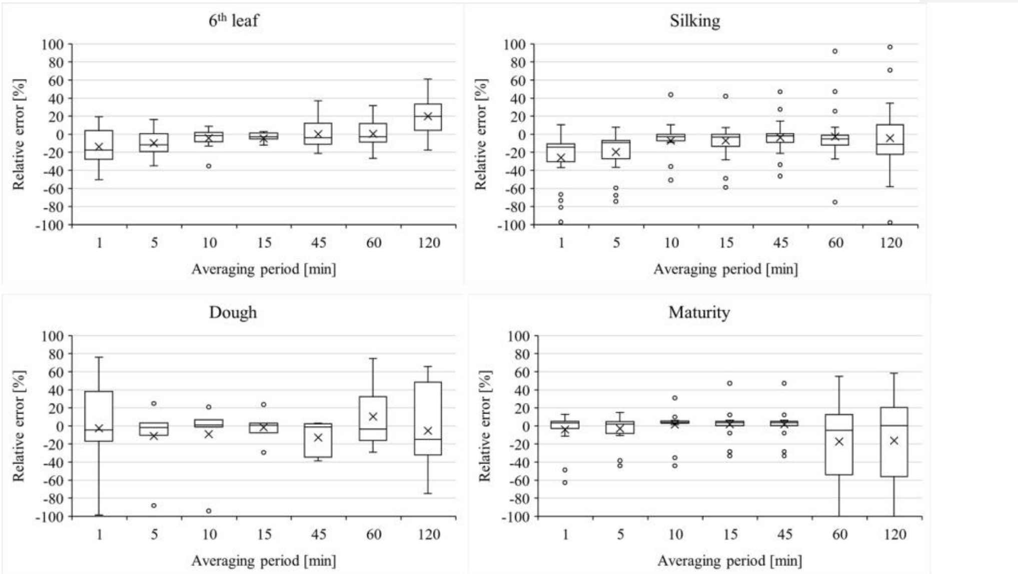

Figure 4a: Whisker plots showing the distribution of error in estimating carbon fluxes with various averaging periods relative to the conventional 30 min averaging.

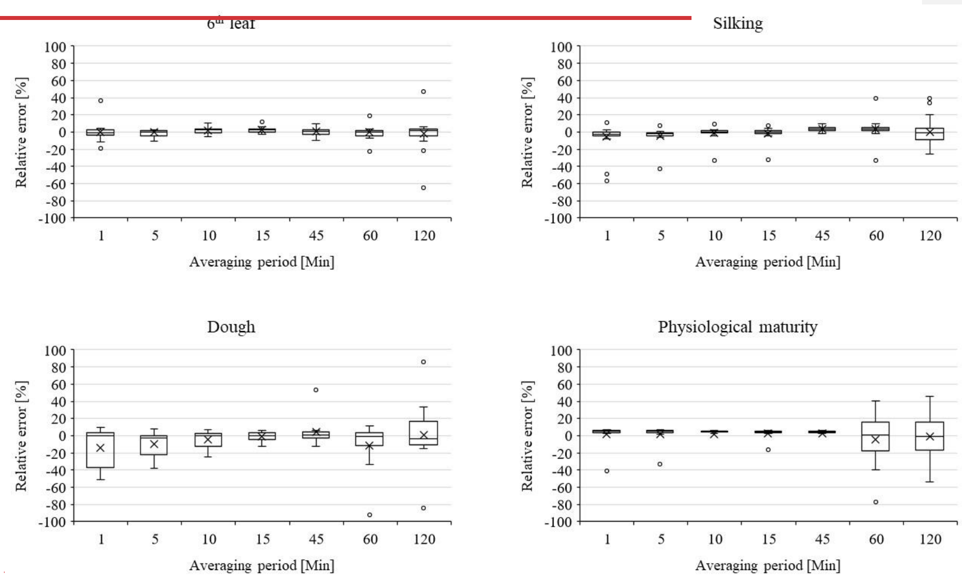

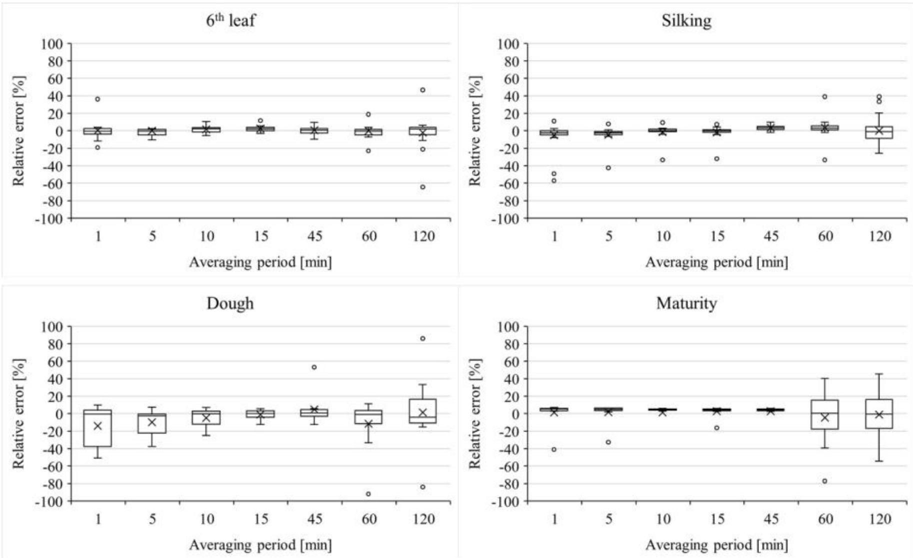

Figure 4b: Whisker plots showing the distribution of error in estimating water fluxes with various averaging periods relative to the conventional 30 min averaging.

3.3 Selection of Optimal averaging period

Ogive functions representing the cumulative integral of the co-spectral energy starting with highest frequency, i.e., 0.016 Hz (T = 1 min) for carbon, water and ~~water~~ WUE fluxes are presented

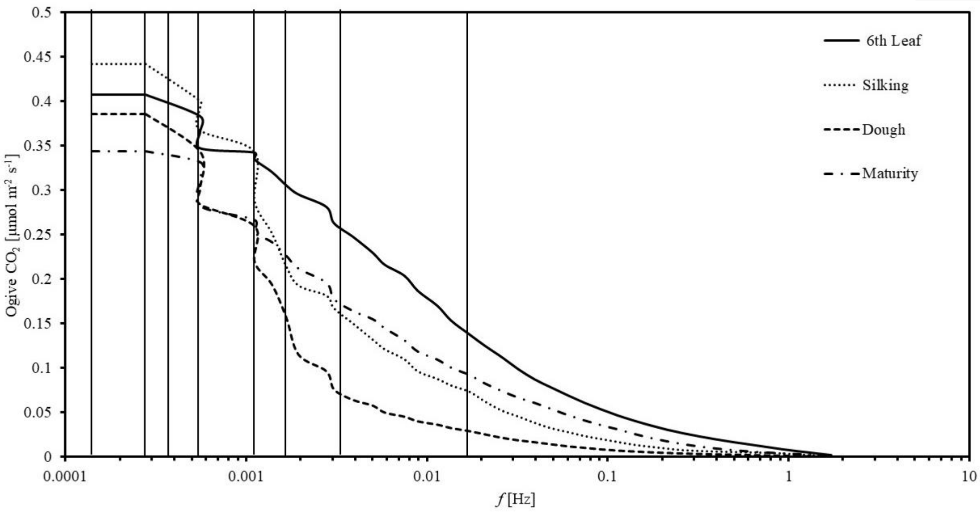

Figure 5a: Ogive plots of carbon fluxes for different growth stages of the Maize crop. (Solid verticals from left to right extremes correspond to the averaging periods of 120 min, 60 min, 45 min, 30 min, 15 min, 10 min, 5min and 1 min respectively).

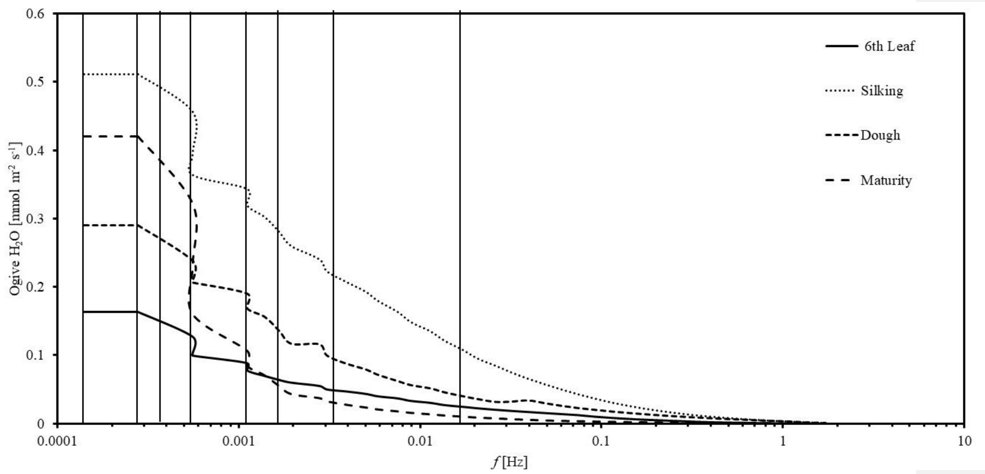

Figure 5b: Ogive plots of water fluxes for different growth stages of the Maize crop. (Solid verticals from left to right extremes correspond to the averaging periods of 120 min, 60 min, 45 min, 30 min, 15 min, 10 min, 5min and 1 min respectively)

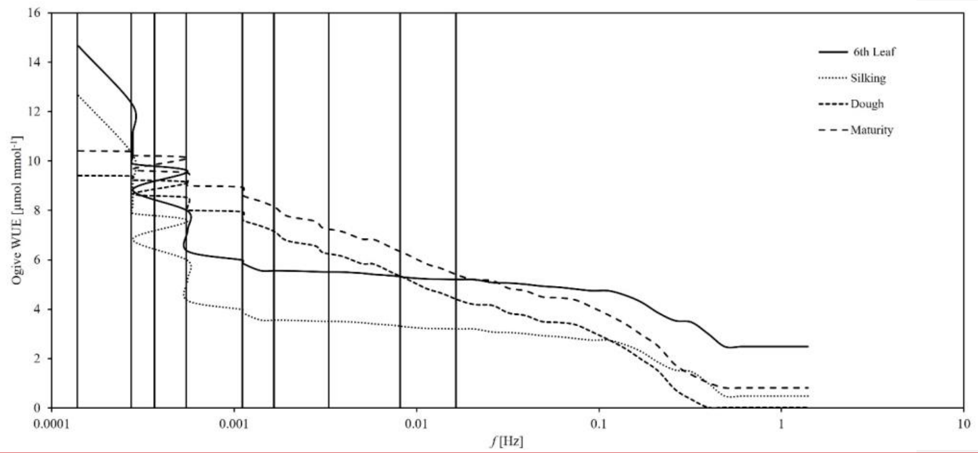

Figure 5c: Ogive plots of water use efficiency for different growth stages of the Maize crop. (Solid verticals from left to right extremes correspond to the averaging periods of 120 min, 60 min, 45 min, 30 min, 15 min, 10 min, 5min and 1 min respectively)

in Figure 5. Shorter time periods corresponding to daytime unstable atmospheric conditions (08:00 am to 04:00 pm) for various growth stages were investigated. Ogive plots of carbon fluxes for 6^{th} leaf and silking stages showed an increasing trend upto 0.011 Hz (15 min) and remained fairly constant before 0.0055 Hz (30 min). This concludes that whole turbulent spectrum can be covered with 15 to 30 min averaging, with negligible flux contribution from longer frequencies. Ogive plots of carbon fluxes for dough and maturity stages showed a continuous increasing trend without a defined plateau (horizontal asymptote) in between. This conclude that the conventional 30 min averaging period is inadequate to capture the low frequency fluxes, thus demanding for higher averaging periods. We observed a similar behaviour with water fluxes (Figure 5b). The flat part of the Ogive curve representing the optimal averaging period was found to vary across the crop cycle. While 15-30 min time-average is suitable for aggregating the EC fluxes during 6^{th} leaf and silking stages, 45-60 min averaging is more appropriate for dough and maturity stages. Similar to carbon and water fluxes, the ogive plots for WUE were presented in Figure 5c. From this, it is observed that the flat part of ogive is achieved at 15 min time average period for the stages of 6^{th} leaf and silking and 45 min time average for the dough and maturity stages which is similar to the carbon and water fluxes. It concludes that the WUE followed a similar behaviour as its individual fluxes i.e. carbon and water fluxes in achieving optimal time averages. The crop biophysical factors like LAI and plant height are minimum during 6^{th} leaf and silking stages contributes low quantity of CO_2 and H_2O fluxes (refer figure 3a & 3b) whereas they are maximum in the later stages of the crop i.e., ~~tasselling~~ dough and maturity by contributing to high quantitiesy of CO_2 and H_2O fluxes (refer figure 3a & 3b). Our results are in accordance with the previous studies of Fong et al., 2020 on Cotton, where the responses in NPP and ET were related seasonally to plant growth stages. The previous studies on various crops revealed that the ~~GPP~~ NPP and ET fluxes were initially low in the early stages and increases towards maturity stage due to crop phenology and management practices. To capture these low quantity fluxes, low averaging periods i.e., 15 min is sufficient, whereas 45 min time-averaging period can capture high quantity fluxes that are prevalent during later growth stages of the crop. As the crop characteristics are dependent on ~~the~~ crop growth stages, a single time-averaging period is not appropriate to capture the dynamics of CO_2 and H_2O fluxes ~~and~~ as well as their ratio WUE. This clearly demonstrates that, as the plant achieves its higher stage, flux contribution from low-frequency components becomes more valuable. Very low averaging periods (ex: 1 min, 5 min) were found unsuitable to capture low-frequency flux components, which is in agreement with literature (Feng, 2017).

3.4 Dynamics of Water use efficiency

Daily means of water use efficiency (WUE) estimated with conventional 30 min and growth specific optimal averaging periods is presented in Figure 6. Mean WUE fluxes for 6th

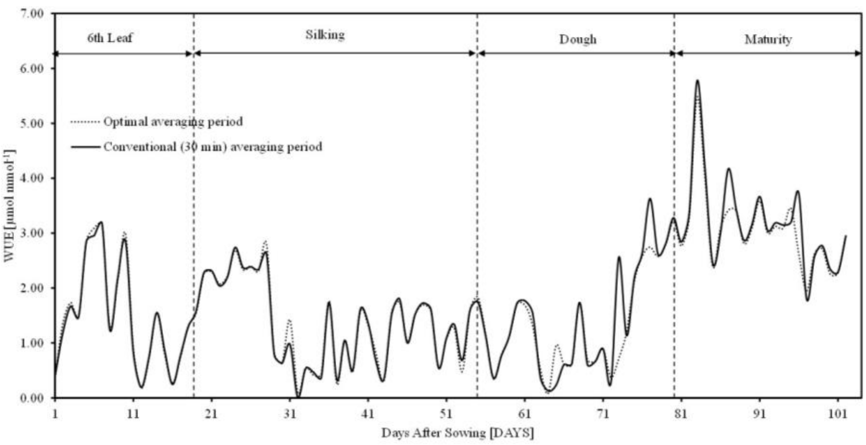

Figure 6: Seasonal variations in daily mean WUE fluxes obtained with conventional 30 min (~~black~~solid) and optimal averaging periods (~~red~~dotted) during the crop cycle.

leaf, silking, dough and maturity stages with conventional 30 min averaging are 1.48 ± 0.96, 1.36 ± 0.73, 1.38 ± 0.95 and 3.184 ± 0.78 µmol mmol^{-1} respectively. Corresponding fluxes with stage specific optimal averaging periods are 1.49 ± 0.95, 1.37 ± 0.74, 1.39 ± 0.79 and 3.06 ± 0.69 µmol mmol^{-1} respectively. Error in estimating mean daily WUE fluxes with 30 min averaging is very low (< 1.45%) during 6th leaf and silking stages, low (8.56 to 9.04 %) during maturity stage, and is moderate (11.84 to 12.12 %) during dough stage. This conclude that, choice of optimal averaging period is more crucial for late stage growth periods of the crop. Distribution of error in estimating WUE fluxes with various averaging periods relative to conventional 30 min average period (RE) is presented in Figure 7. A close to zero RE with all averaging periods during 6th leaf and silking stages conclude that, choice of averaging period has insignificant role in estimating the WUE fluxes, particularly during early growth stages. A slightly high RE (~ -5.4%) during dough and maturity stages conclude that, choice of averaging period matters for WUE estimation during late stage periods. Hence, conventional 30 min averaging period can be considered for estimating WUE fluxes during 6th leaf and silking stages, whereas optimal averaging period need to be considered for estimating WUE fluxes during dough and maturity stages. Correlation charts showing the linear association within carbon, water, and WUE fluxes represented at different averaging periods is presented in Figure 8. For ease with comparison, data for the entire crop cycle was considered. Linear association

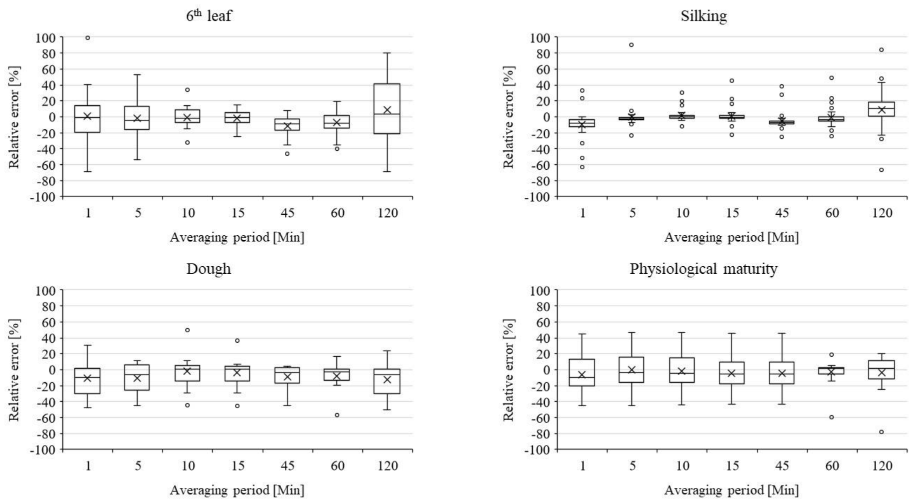

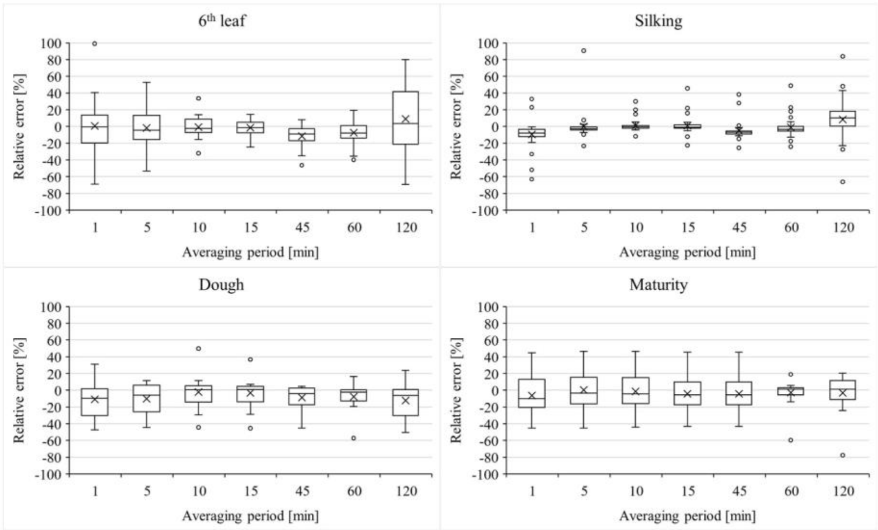

Figure 7: Whisker plots showing the distribution of error in estimating WUE fluxes with various averaging periods relative to the conventional 30 min averaging.

between any two averaging periods is positive (ρ > 0.56) for carbon and water fluxes. Except with 120 min time-averaging, all other averaging periods are strongly correlated (ρ > 0.87) with 30 min averaging period. However, a poor linear association in WUE fluxes was observed between any two averaging periods, which is attributed to a larger variation in individual WUE fluxes between averaging periods. However, the corresponding individual carbon and water fluxes have recorded low variations between time averages. This conclude that, the need for optimal averaging period is more crucial in estimating WUE fluxes rather than individual carbon and water fluxes. Our findings can improve representation of WUE fluxes using EC data, thereby help in developing efficient water management strategies in response to WUE changes.

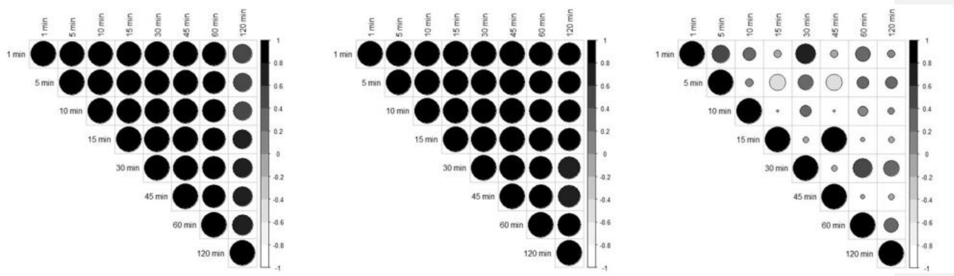

Figure 8: Correlation charts showing the linear association of **a**) Carbon fluxes, **b**) Water fluxes, and **c**) WUE fluxes estimated with different averaging periods.

4.0 CONCLUSIONS

This study explores the effect of averaging period of EC fluxes on EBR dynamics and WUE in semi-arid Indian conditions. The proposed methodology was applied on drip-irrigated M~~m~~aize field for one crop period (May-Sept 2019). Major findings of this study are:

- EBR was found vary marginally at low averaging periods and less significant during higher averaging periods.
- With reference to conventional 30 min averaging period, relative error is within 12% for 10-45 min averaging periods for carbon fluxes and is within 5% for 15-45 averaging periods for water fluxes.
- From ogive analysis we found the optimal averaging period as 15 - 30 min for the 6th leaf, and silking stages, and as 45 – 60 min for the dough and maturity stages.
- The mean carbon fluxes are increasing from 1.81 ± 0.06 μmol^{+1}m^{-2}s^{-1} (6th leaf stage) to 15.44 ± 0.75 μmol^{+1}m^{-2}s^{-1} (maturity stage) which indicates that carbon sink is a function of crop growth period. In case of water fluxes, it increased from 2.52 ± 0.13 mmol^{+1}m^{-2}s^{-1} (6th leaf stage) to 5.02 ± 0.29 mmol^{+1}m^{-2}s^{-1} (maturity stage). Variation of carbon and water fluxes are directly influencing WUE dynamics.
- The variation in WUE was increased subsequently with the plant growth and achieved its maximum value of 5.17 μmol mmol^{-1} in between dough to maturity stages which concludes that, crop consumes more carbon than water as the crop period progresses.
- The correlation between CO_2 and H_2O fluxes for all averaging periods was found to be high. However, WUE, which is calculated as the ratio of CO_2 and H_2O fluxes, is not following the same pattern. While 45 min and 15 min averaged WUE exhibits a good correlation, 30 min averaged WUE is not correlated with other averaging periods. Averaging period is found to be an influencing factor in controlling WUE, hence should be considered with caution during the crop growth.

This study is limited to understand the role of different time-averaging periods on EC observed carbon, water fluxes as well as EC derived WUE fluxes contributed by homogeneous Maize crop which is having relatively smaller flux footprint in an unstable atmospheric condition. ~~This study is limited to understand the role of different time-averaging periods on EC observed~~

Formatted: Font: (Default) Times New Roman, 12 pt, Not Highlight

Formatted: Space After: 0 pt

~~carbon, water fluxes as well as EC derived WUE fluxes~~. Study findings can help to accurately characterise WUE of Maize crop considering growth stages for effective implementation of irrigation strategies.

Formatted: Font color: Red

Acknowledgments

The authors acknowledge the anonymous reviewers for their insightful comments. This research evolved as an extension of a term project in CE6520-Irrigation Water Management course at IIT Hyderabad.

Data Availability Statement:

All footprint climatologies, site-level data files, and supplementary material can be accessed via the Zenodo Data Repository (https://zenodo.org/badge/latestdoi/528291820) (Shweta07081992, 2022)

Author Contribution:

Arun Rao Karimindla: Data processing and Analysis, Writing- Original draft. **Shweta Kumari:** Conceptualization, Methodology, Project Supervision. **Saipriya SR**: Data processing Analysis, and Writing- Original draft. **Syam Chintala:** Data processing and Analysis, Writing- Original draft. **BVN Phanindra Kambhammettu:** Project Administration, Writing- Reviewing and Editing.

Competing interests:

The authors declare that they have no known competing interests or personal relationships that could have appeared to influence the work reported in this paper.

5.0 REFERENCES

Barr, A. G., Morgenstern, K., Black, T. A., McCaughey, J. H., & Nesic, Z. (2006). Surface energy balance closure by the eddy-covariance method above three boreal forest stands and implications for the measurement of the CO2 flux. Agricultural and Forest Meteorology, 140(1–4), 322–337. https://doi.org/10.1016/j.agrformet.2006.08.007

Bramley, H., Turner, N. C., & Siddique, K. H. M. (2013). Water Use Efficiency. In C. Kole (Ed.), Genomics and Breeding for Climate-Resilient Crops: Vol. 2 Target Traits (pp. 225–268). Springer Berlin Heidelberg. https://doi.org/10.1007/978-3-642-37048-9_6

Berger, B. W., Davis, K. J., Yi, C., Bakwin, P. S., & Zhao, C. L. (2001). Long-term carbon dioxide fluxes from a very tall tower in a northern forest: Flux measurement methodology. Journal of Atmospheric and Oceanic Technology, 18(4), 529–542.

Central Ground Water Board. (2015). Annual Report 2013. https://cgwb.gov.in/old_website/Annual-Reports/Annual Report-2013-14.pdf

Charuchittipan, D., W. Babel, M. Mauder, J. P. Leps, and T. Foken, 2014: Extension of the Averaging Time in Eddy-Covariance Measurements and Its Effect on the Energy Balance Closure. *Boundary-Layer Meteorol.*, **152**, 303–327, https://doi.org/10.1007/s10546-014-9922-6.

Chen, Y. Y., and M. H. Li, 2012: Determining adequate averaging periods and reference coordinates for eddy covariance measurements of surface heat and water vapor fluxes over mountainous terrain. *Terr. Atmos. Ocean. Sci.*, **23**, 685–701, https://doi.org/10.3319/TAO.2012.05.02.01(Hy).

Chintala, S., Karimindla, A. R., & Kambhammettu, B. V. N. P. (2024). Scaling relations between leaf and plant water use efficiencies in rainfed Cotton. Agricultural Water Management, 292, 108680. https://doi.org/https://doi.org/10.1016/j.agwat.2024.108680

Desjardins, R. L., MacPherson, J. I., Schuepp, P. H., & Karanja, F. (1989). An evaluation of aircraft flux measurements of CO2, water vapor and sensible heat. Boundary-Layer Meteorology, 47(1), 55–69. https://doi.org/10.1007/BF00122322

Eshonkulov, R., and Coauthors, 2019: Evaluating multi-year, multi-site data on the energy balance closure of eddy-covariance flux measurements at cropland sites in southwestern Germany. *Biogeosciences*, **16**, 521–540, https://doi.org/10.5194/bg-16-521-2019.

Feng, J., B. Zhang, Z. Wei, and D. Xu, 2017: Effects of Averaging Period on Energy Fluxes and the Energy-Balance Ratio as Measured with an Eddy-Covariance System. *Boundary-Layer Meteorol.*, **165**, 545–551, https://doi.org/10.1007/s10546-017-0284-8.

Ficci, 2014: Maize in India. *India Maize Summit'14*, 1–32.

~~Finkelstein, P. L., T. Park, N. Carolina, and F. Sims, 2001: z [(w ' O ') Fc. **106**, 3503–3509.~~

Finkelstein, P. L., & Sims, P. F. (2001). Sampling error in eddy correlation flux measurements. Journal of Geophysical Research, 106, 3503–3509. https://api.semanticscholar.org/CorpusID:128980052

Finnigan, J. J., 2004: A re-evaluation of long-term flux measurement techniques part II: Coordinate systems. *Boundary-Layer Meteorol.*, **113**, 1–41, https://doi.org/10.1023/B:BOUN.0000037348.64252.45.

Finnigan, J. J., R. Clement, Y. Malhi, R. Leuning, and H. A. Cleugh, 2003: Re-evaluation of long-term flux measurement techniques. Part I: Averaging and coordinate rotation. *Boundary-Layer Meteorol.*, **107**, 1–48, https://doi.org/10.1023/A:1021554900225.

Foken, T., and B. Wichura, 1996: Tools for quality assessment of surface-based flux measurements. *Agric. For. Meteorol.*, **78**, 83–105, https://doi.org/10.1016/0168-1923(95)02248-1.

Foken, T., Göockede, M., Mauder, M., Mahrt, L., Amiro, B., & Munger, W. (2005). Post-Field Data Quality Control BT - Handbook of Micrometeorology: A Guide for Surface Flux Measurement and Analysis (X. Lee, W. Massman, & B. Law, Eds.; pp. 181–208). Springer Netherlands. https://doi.org/10.1007/1-4020-2265-4_9

Foken, T., M. Aubinet, J. J. Finnigan, M. Y. Leclerc, M. Mauder, and K. T. Paw U, 2011: Results of a panel discussion about the energy balance closure correction for trace gases. *Bull. Am. Meteorol. Soc.*, **92**, https://doi.org/10.1175/2011BAMS3130.1.

Fong, B. N., Reba, M. L., Teague, T. G., Runkle, B. R. K., & Suvočarev, K. (2020). Eddy covariance measurements of carbon dioxide and water fluxes in US mid-south cotton production. Agriculture, Ecosystems and Environment, 292. https://doi.org/10.1016/j.agee.2019.106813

Gao, Z., H. Liu, G. G. Katul, and T. Foken, 2017: Non-closure of the surface energy balance explained by phase difference between vertical velocity and scalars of large atmospheric eddies. *Environ. Res. Lett.*, **12**, https://doi.org/10.1088/1748-9326/aa625b.

Gerken, T., and Coauthors, 2018: Investigating the mechanisms responsible for the lack of surface energy balance closure in a central Amazonian tropical rainforest. *Agric. For. Meteorol.*, **255**, 92–103, https://doi.org/10.1016/j.agrformet.2017.03.023.

Kidston, J., Brümmer, C., Black, T. A., Morgenstern, K., Nesic, Z., McCaughey, J. H., &

Barr, A. G. (2010). Energy balance closure using eddy covariance above two different land surfaces and implications for CO2 flux measurements. Boundary-Layer Meteorology, 136(2), 193–218. https://doi.org/10.1007/s10546-010-9507-y

Kole, C., 2013: *Genomics and breeding for climate-resilient crops: Vol. 2 target traits*. 1–474 pp.

Kottek, M., J. Grieser, C. Beck, B. Rudolf, and F. Rubel, 2006: World map of the Köppen-Geiger climate classification updated. *Meteorol. Zeitschrift*, **15**, 259–263, https://doi.org/10.1127/0941-2948/2006/0130.

Leclerc, M. Y., and T. Foken, 2014: *Footprints in micrometeorology and ecology*. Springer,.

Lee, X., Q. Yu, X. Sun, J. Liu, Q. Min, Y. Liu, and X. Zhang, 2004: Micrometeorological fluxes under the influence of regional and local advection: A revisit. *Agric. For. Meteorol.*, **122**, 111–124, https://doi.org/10.1016/j.agrformet.2003.02.001.

Leuning, R., E. van Gorsel, W. J. Massman, and P. R. Isaac, 2012: Reflections on the surface energy imbalance problem. *Agric. For. Meteorol.*, **156**, 65–74, https://doi.org/10.1016/j.agrformet.2011.12.002.

Malhi, Y., K. McNaughton, and C. Von Randow, 2004: Low Frequency Atmospheric Transport and Surface Flux Measurements. 101–118, https://doi.org/10.1007/1-4020-2265-4_5.

Manon, M., and M. Kristian, 2020: Estimating local atmosphere-surface fluxes using eddy covariance and numerical Ogive optimization. **15**, 21387–21432, https://doi.org/10.5194/acpd-14-21387-2014.

Mauder, M., and T. Foken, 2006: Impact of post-field data processing on eddy covariance flux estimates and energy balance closure. *Meteorol. Zeitschrift*, **15**, 597–609, https://doi.org/10.1127/0941-2948/2006/0167.

Medrano, H., and Coauthors, 2015: From leaf to whole-plant water use efficiency (WUE) in complex canopies: Limitations of leaf WUE as a selection target. *Crop J.*, **3**, 220–228, https://doi.org/10.1016/j.cj.2015.04.002.

Oncley, S. P., and Coauthors, 2007: The energy balance experiment EBEX-2000. Part I: Overview and energy balance. *Boundary-Layer Meteorol.*, **123**, 1–28, https://doi.org/10.1007/s10546-007-9161-1.

Peddinti, S. R., and B. P. Kambhammettu, 2019: Dynamics of crop coefficients for citrus orchards of central India using water balance and eddy covariance flux partition techniques. *Agric. Water Manag.*, **212**, 68–77, https://doi.org/10.1016/j.agwat.2018.08.027.

Peddinti, S. R., Kambhammettu, B. V. N. P., Rodda, S. R., Thumaty, K. C., & Suradhaniwar, S. (2020). Dynamics of Ecosystem Water Use Efficiency in Citrus Orchards of Central India Using Eddy Covariance and Landsat Measurements. Ecosystems, 23(3), 511–528. https://doi.org/10.1007/s10021-019-00416-3

Reed, D. E., J. M. Frank, B. E. Ewers, and A. R. Desai, 2018: Time dependency of eddy covariance site energy balance. *Agric. For. Meteorol.*, **249**, 467–478, https://doi.org/10.1016/j.agrformet.2017.08.008.

Sakai, R. K., D. R. Fitzjarrald, and K. E. Moore, 2001: Importance of low-frequency contributions to eddy fluxes observed over rough surfaces. *J. Appl. Meteorol.*, **40**, 2178–2192, https://doi.org/10.1175/1520-0450(2001)040<2178:IOLFCT>2.0.CO;2.

Sharma, B. R., Gulati, Mohan, Gayathri, Manchanda, S., Ray, I., & Amarasinghe, U. (2018). Water Productivity Mapping of Major Indian Crops. NABARD and ICRIER, 4(1), 88–100.

Shankar, V., C. S. P. Ojha, and K. S. H. Prasad, 2012: Irrigation Scheduling for Maize and Indian-mustard based on Daily Crop Water Requirement in a Semi- Arid Region. **6**, 476–485.

Soujanya, B., B. B. Naik, M. U. Devi, T. L. Neelima, and A. Biswal, 2021: Dry Matter Production and Nitrogen Uptake as Influenced by Irrigation and Nitrogen Levels in Maize. *Int. J. Environ. Clim. Chang.*, 155–161, https://doi.org/10.9734/ijecc/2021/v11i1130528.

Sun, X. M., Z. L. Zhu, X. F. Wen, G. F. Yuan, and G. R. Yu, 2006: The impact of averaging period on eddy fluxes observed at ChinaFLUX sites. *Agric. For. Meteorol.*, **137**, 188–193, https://doi.org/10.1016/j.agrformet.2006.02.012.

Tang, X., Z. Ding, H. Li, X. Li, J. Luo, J. Xie, and D. Chen, 2015: Characterizing ecosystem water-use efficiency of croplands with eddy covariance measurements and MODIS products. *Ecol. Eng.*, **85**, 212–217, https://doi.org/10.1016/j.ecoleng.2015.09.078.

Tong, X., J. Zhang, P. Meng, J. Li, and N. Zheng, 2014: Ecosystem water use efficiency in a warm-temperate mixed plantation in the North China. *J. Hydrol.*, **512**, 221–228, https://doi.org/10.1016/j.jhydrol.2014.02.042.

Tong, X. J., J. Li, Q. Yu, and Z. Qin, 2009: Ecosystem water use efficiency in an irrigated cropland in the North China Plain. *J. Hydrol.*, **374**, 329–337, https://doi.org/10.1016/j.jhydrol.2009.06.030.

Twine, T. E., and Coauthors, 2000: Correcting eddy-covariance flux underestimates over a grassland. *Agric. For. Meteorol.*, **103**, 279–300, https://doi.org/10.1016/S0168-1923(00)00123-4.

~~Vickers, D., and L. Mahrt, 1997: graphDBSummary. *J. Atmos. Ocean. Technol.*, **14**, 512–526.~~

Vickers, D., & Mahrt, L. (1997). Quality control and flux sampling problems for tower and aircraft data. Journal of Atmospheric and Oceanic Technology, 14(3), 512–526. https://doi.org/10.1175/1520-0426(1997)014<0512:QCAFSP>2.0.CO;2

Wang, X., C. Wang, and B. Bond-Lamberty, 2017: Quantifying and reducing the differences in forest CO2-fluxes estimated by eddy covariance, biometric and chamber methods: A global synthesis. *Agric. For. Meteorol.*, **247**, 93–103, https://doi.org/10.1016/j.agrformet.2017.07.023.

Wilson, K., E. Falge, M. Aubinet, and D. Baldocchi, 2002: DigitalCommons @ University of Nebraska - Lincoln Energy Balance Closure at FLUXNET Sites. *Agric. For. Meteorol.*, 223–243.

Zhang, P., G. Yuan, and Z. Zhu, 2013: Determination of the averaging period of eddy covariance measurement and its influences on the calculation of fluxes in desert riparian forest. *Arid L. Geogr.*, **36**, 401–407.